9th International Operational Modal Analysis Conference
iomac
July 3 - 6, 2022
Vancouver, Canada

A GENERAL FRAMEWORK FOR DAMAGE DETECTION WITH STATISTICAL DISTANCE MEASURES: APPLICATION TO CIVIL ENGINEERING STRUCTURES

Niels-Jørgen Jacobsen[1], Palle Andersen[2], Alexander Mendler[3], Szymon Greś[4]

[1] Product Manager – Structural Dynamics Solutions, Hottinger Brüel & Kjær A/S, 2830 Virum, Denmark
[2] Managing Director, Structural Vibration Solutions A/S, NOVI Science Park, 9220 Aalborg, Denmark
[3] Postdoctoral Fellow, Technical University of Munich, TUM School of Engineering and Design, 80333 Munich, Germany
[4] Postdoc, Institute of Structural Engineering (IBK), SMM team, ETH Zürich, 8093 Zürich, Switzerland

ABSTRACT

Detecting damage in structural systems is often achieved by a statistical comparison of damage-sensitive characteristics of a structure evaluated on baseline data, against the corresponding characteristics obtained using data collected from a potentially defective structure. While several vibration-based methods have been proposed and successfully applied to detect damage in both mechanical and civil structures over the past years, the general framework describing their common properties and unifying the statistical decision about damage has mainly been elaborated in the control community. In this paper, we revise this framework in the context of detecting damage in structural systems. The statistical properties of three commonly used damage detection methods are recalled, and it is shown that their evaluation for damage boils down to a simple statistical distance. The framework is adopted to a commercial structural health monitoring software suite and its practical merit is illustrated on damage detection of two full-scale highway bridges.

Keywords: Damage detection, squared Mahalanobis distance, subspace methods, mode tracking, control chart, Structural Health Monitoring, Operational Modal Analysis

1. INTRODUCTION

Vibration-based damage detection refers to detecting damage through changes in a set of features extracted from the vibration signals collected from structural health monitoring (SHM) systems. Over the past decade, it became an effective methodology in triggering on-demand inspections after damaging events in large-scale civil and mechanical structures, e.g., wind turbines [1,2], offshore structures [3,4], and bridges [5,6]. It remains the sole aspect of the SHM triad, i.e., damage detection, localization, and quantification, that has been implemented in commercial software such as ARTeMIS Modal Pro [7] and PULSE™ Operational Modal Analysis [8].

In the field of fault diagnosis of mechanical systems, myriads of different vibration-based damage detection methods exist; see [9] for a review of early developments. Commercially available methods often use the modal approach, which presumes that the damage is manifested through a change in the modal parameters, i.e., the natural frequencies, damping ratios and mode shapes. The modal parameters are typically identified from measured data and compared to baseline values using statistical distance measures. However, some field work questions the use of the modal parameters as damage-sensitive features, arguing that they are not sensitive enough to identify local faults [1,2], especially if the structure is only excited by low-frequency inputs. One bypass to the modal framework employed in the commercial software, is to use the statistical fault detection and isolation methods [10,11], where the damage-sensitive features of the system are derived directly from measured data and comprise, e.g., angles between dynamic signal spaces, and are evaluated for damage in statistical hypothesis tests. While efficient in detecting damage, the practical use and interpretation of the latter methodology is often hindered by its complex mathematical formulation.

The goal of this paper is to illustrate that the current commercial practice for the vibration-based damage detection boils down to a simple statistical distance obtained from a residual evaluated between some baseline (reference) features of the system and the features from the currently tested data. In this context, three damage detection residuals are investigated, namely, the classic subspace-based residual [12], the robust subspace-based residual [10], and the modal parameter-based residual [13]. Each metric is calculated based on vibration data collected during normal operating conditions, and the damage is denoted as deviations of the distance measure from the reference state. The considered methods are implemented in the modal analysis and structural health monitoring software packages ARTeMIS Modal and PULSE Operational Modal Analysis, in which their joint features are concluded in a control chart to enhance the resolution of the damage detection. Methods are evaluated based on the ambient vibration signals from two benchmark structures, that is, the Z24 bridge in Switzerland and the S101 bridge in Austria. The results reveal that the performance of the damage detection methods is similar and the fusion of the damage indicators in the control chart provides the most accurate view on the progressively damaged systems. The paper is organized as follows: Section 2 recaps the statistical tests for damage detection, Section 3 contains two cases studies and Section 4 discusses the results.

2. METHODOLOGY

In this section, the background on output-only vibration analysis of mechanical systems is recalled, the definition of three different damage detection residuals is outlined and the general framework for the statistical decision-making about damage is stated.

2.1. Background

A fundamental step in damage detection is the evaluation of the dynamic features of the system from monitoring data, so that their changes can be related to the occurrence of damage. To this end, many classical features used for damage detection originate from system identification and comprise, e.g., subspace characteristics of data matrices, or modal parameters, where both can be obtained from the response measurements, e.g., accelerations, velocities, displacements, inclinations, or strains.

Consider N acceleration measurements $y = [y_1 \dots y_N]^T \in \mathrm{R}^{r\mathrm{x}N}$ collected using r sensors sampling the dynamic response of the monitored linear time-invariant (LTI) dynamic system with a sampling frequency f_s. The covariance matrix of the output measurements $R_i = \mathrm{E}\left(y_{k+i}\mathrm{y}_{\mathrm{k}}^{\mathrm{T}}\right) \in \mathrm{R}^{rxr}$ can be structured in the block-Hankel matrix $H \in \mathrm{R}^{(p+1)r\,x\,qr}$ as follows:

$$H = \begin{bmatrix} R_1 & R_2 & \cdots & R_q \\ R_2 & R_3 & \dots & R_{q+1} \\ \vdots & \vdots & \ddots & \vdots \\ R_{p+1} & R_{p+2} & \dots & R_{p+q} \end{bmatrix}, \tag{1}$$

where p and $q = p + 1$ are the parameters that denote the memory of the system. The factorization of H to some low-rank matrices fully describing the dynamics of the underlying LTI mechanical system is the cornerstone for obtaining the damage-sensitive features in the SHM methods considered in this paper. Assume that the order of the system *n=2m* is known, where *m* is the number of modal parameters observed in the considered frequency band. The singular value decomposition (SVD) of H writes:

$$H = [U_1 \quad U_2] \begin{bmatrix} D_1 & 0 \\ 0 & D_2 \end{bmatrix} \begin{bmatrix} V_1^T \\ V_2^T \end{bmatrix}, \tag{2}$$

where $U_1 \in \mathrm{R}^{(p+1)r\,x\,n}$ and $V_1 \in \mathrm{R}^{qr\,x\,n}$ are called the image and the co-image of a matrix, respectively, and correspond to a collection of *n* left and right singular vectors related to *n* singular values $D_1 \in \mathrm{R}^{n\,x\,n}$. The matrices $U_2 \in \mathrm{R}^{(p+1)r\,x\,(p+1)r-n}$ and $V_2 \in \mathrm{R}^{qr\,x\,qr-n}$ are called the left and right nullspace of a matrix, respectively. They contain the left and right singular vectors that correspond to the singular values in $D_2 \in \mathrm{R}^{(p+1)r-n\,x\,qr-n}$ which approximate zero. Their use in the context of the considered damage detection methodology is elaborated in Sections 2.2.1 - 2.2.3.

2.2. Damage detection residuals

Let ζ denote a damage detection residual obtained from some damage-sensitive features extracted from the measurement data in the reference and in the currently tested state and let Σ_ζ be its asymptotic covariance matrix. To compare the measurements from the healthy and the tested states, the residual is expressed to follow a Gaussian distribution, whose mean value is zero if the features of the currently tested system statistically correspond to the baseline features and is different from zero otherwise. The definition of the residual depends on the chosen damage detection method. A brief description of the damage detection residuals used in this paper is enclosed below. For brevity, only the definition of residuals is outlined and not their statistical characteristics, e.g., covariance computation. Regarding this, the interested reader is encouraged to refer to the references enclosed in the respective sections.

2.2.1. Classic subspace-based residual

The classic subspace-based damage detection residual is defined as a product of a Hankel matrix evaluated from the test data H^{test} and the left nullspace of the Hankel matrix obtained from the baseline data U_2^{ref} [12]. The resultant residual can be written as:

$$\zeta = \sqrt{N}\, U_2^{ref^T} H^{test}. \tag{3}$$

After the left nullspace property, i.e., $U_2^{\mathrm{ref}^T} H^{\mathrm{test}} \to 0$, when the test data statistically corresponds to the baseline data, the mean value of the residual (3) is zero when the currently tested data set is classified healthy, and it is different from zero when the currently tested data is collected from a damaged structure.

2.2.2. Robust subspace-based residual

The robust subspace-based residual is defined from a product of images of a Hankel matrix evaluated from the test data $U^{\mathrm{test}} = U_1^{\mathrm{test}}(U_1^{\mathrm{test}})^T$ and the left nullspace of the Hankel matrix obtained from the baseline data U_2^{ref} [10]. The resultant residual can be written as:

$$\zeta = \sqrt{N}\, U_2^{\mathrm{ref}^T} U^{\mathrm{test}}. \tag{4}$$

Like the classic residual, the mean value of the robust residual is zero when the features obtained from the currently tested data corresponds to the baseline features and it is different from zero otherwise. The benefit of using the image product U^{test} in (4) compared to H^{test} in (3) is that U^{test} is not heavily affected by the noise properties of the singular values and the right singular vectors; a clear drawback is its additional computational complexity related to the computation of the covariance matrix.

2.2.3. Modal parameter-based residual

The modal parameter-based residual is defined as the difference between currently estimated modal parameters and their reference values obtained from data in a baseline state [13]. Let x^{ref} and x^{test} contain a stacked and vectorized collection of the modal parameter estimates, e.g., the natural frequencies and the mode shapes, obtained from the baseline and the test data using SSI. The modal parameter-based residual is defined as:

$$\zeta = \sqrt{N}(x^{\text{ref}} - x^{\text{test}}), \tag{5}$$

The expected value of the residual is zero when the modal parameter estimates obtained from the currently tested data and the baseline modal parameter estimates converge to the same expected value. Otherwise, the expected value of the residual (5) is different from zero, which signifies the occurrence of damage. The computation of the consistent estimates of the joint covariance of the natural frequencies and the mode shapes can be found, e.g., in [14, 15], and case studies confirming the Gaussian characteristics of modal parameter estimates can be found, e.g., in [16].

2.3. General framework for damage detection

Based on the features extracted from the measurement data in the reference and in the currently tested state, the goal of damage detection is to decide whether there is a significant change between the two states, i.e., whether the expected value of the residual is statistically zero, or not. This decision can be achieved through statistical hypothesis tests, e.g., with Generalized Likelihood Ratio (GLR) test [11], or with some statistical distance measures, e.g., squared Mahalanobis distance [17]. For the residuals considered in this work, the likelihood ratio statistics boils down to the squared Mahalanobis distance, which is used for damage detection in the remainder of this paper.

The squared Mahalanobis distance describes a squared distance between a point and a distribution. The distance is zero if the investigated point is at the mean of the reference distribution, and it is not zero otherwise. As such, the metric:

$$d = \zeta^T {\Sigma_\zeta}^{-1} \zeta, \tag{6}$$

can be considered as a dissimilarity measure. When the residual follows an asymptotically Gaussian distribution with zero mean:

$$\zeta \to \mathrm{N}(0, \Sigma_\zeta), \tag{7}$$

the currently tested data set is classified healthy, since the expected value of the dissimilarity between the baseline features and the tested features is null, and then it is well-known that *d* follows a central χ^2 distribution [17]. When the system has undergone a change and the expected value of the residual is not zero but δ, then

$$\zeta \to \mathrm{N}(\delta, \Sigma_\zeta), \tag{8}$$

the currently tested data set is classified as damaged, and *d* follows a noncentral χ^2 distribution [17].

Residuals (3 - 5) satisfy properties (7 - 8) and consequently can be used for statistical damage diagnosis with the squared Mahalanobis distance (6). To decide about the damage, the value of the distance statistics is compared to a quantile of the distribution of the test derived from the baseline data. This quantile is evaluated for some confidence level α, where 1- α denotes the statistical significance level, i.e., the probability of false alarms to occur. The general premise of this statistical framework is illustrated in Figure 1.

To simplify the decision about damage, the squared Mahalanobis distance statistics obtained from different damage detection residuals are combined in a Hotelling T2 control chart [6]. The control chart statistics are computed from the sample mean and the sample covariance obtained from the test statistics of each damage detection residual.

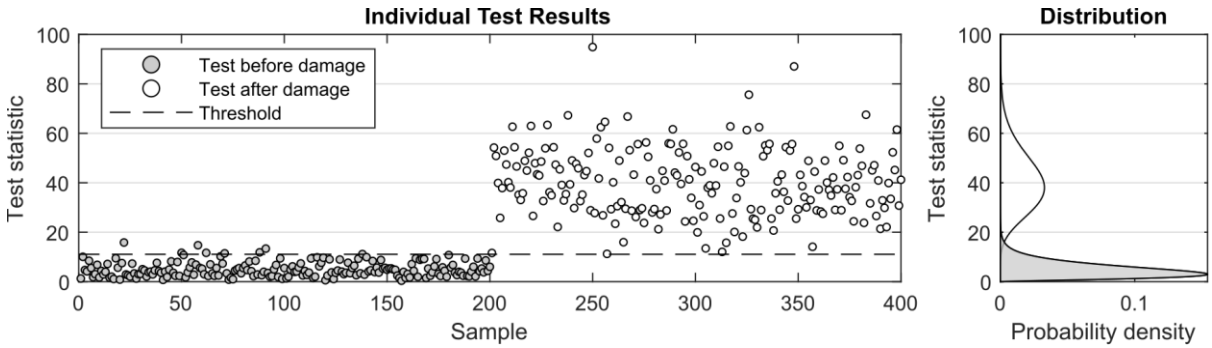

Figure 1. Decision framework for damage detection

3. CASE STUDIES

Below, two case studies on highway bridges are presented.

3.1. Z24 bridge

The Z24 bridge is a benchmark for many studies involving system identification and damage diagnosis [5]. Before its demolition in 1998, a progressive damage campaign was carried out and consisted of a series of ambient and forced vibration tests conducted while inducing different kinds of damage on the bridge. The vibration tests were conducted with 28 moving and 5 fixed sensors measuring vertical, transverse, and lateral accelerations of the bridge. For this study, only the measurements from 5 fixed sensors are analysed. The data acquisition was performed with a sampling frequency of 100 Hz and the length of each measurement was 655 seconds. A total number of 54 data sets were analysed, from which the first 18 measurements were under healthy conditions. Among the first 18 healthy data sets, 6 data sets were selected for the reference state computation. For data sets 19 to 36, measurements were collected after lowering one of the bridge piers by 20 mm. Data sets 37 to 54 were obtained after lowering the same pier by another 20 mm. The view on the bridge with positions and directions of the sensors is shown in Figure 2.

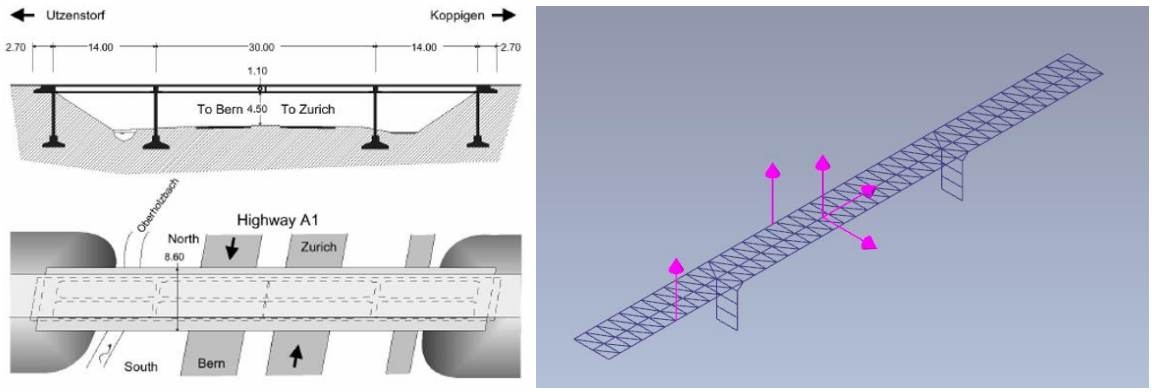

Figure 2. Front and top views of the Z24 bridge (left). Geometry with 5 fixed sensors (right)

The first 9 modes obtained with the Stochastic Subspace Identification – Extended Unweighted Principal Components (SSI–UPCX) method and tracked across the 54 data sets are shown in Figure 3.

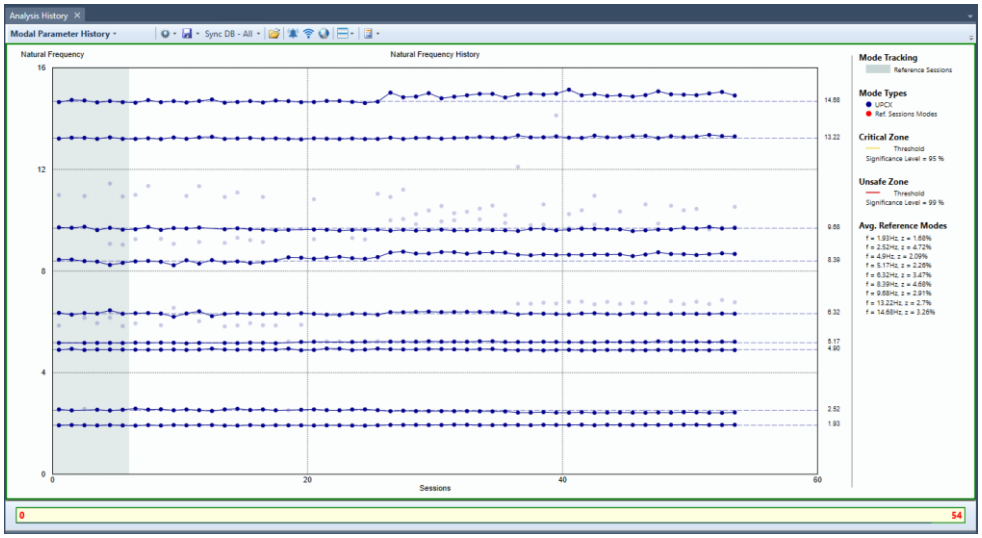

Figure 3. Modal parameters of the Z24 bridge tracked across the 54 data sets. Natural frequencies shown

The mean values of the corresponding natural frequencies and the mode shape estimates obtained over the first 6 data sets are used to establish a baseline (reference) for the modal parameter-based damage detection (5). The remaining 48 data sets are used for damage testing with the squared Mahalanobis distance (6). The resultant damage indicators are presented in Figure 4. Three decision zones are shown. The 'safe zone' is shown with green colour and indicates that the corresponding test values lie within the 95% quantile of the reference distribution statistics, the 'critical zone' shown with yellow colour indicates that the test values lie between the 95% quantile and the 99% quantile of the reference distribution, and the 'unsafe zone' shown with red colour indicates that the corresponding test values exceed the 99% quantile of the reference distribution.

Figure 4 illustrates that one test value corresponding to data collected from the bridge in an undamaged state has exceeded the 99% quantile threshold, falsely alarming damage. This is most likely caused by a missing tracked mode of the fourth and the seventh modes. Overall, however, the damage, after its inception, is well detected.

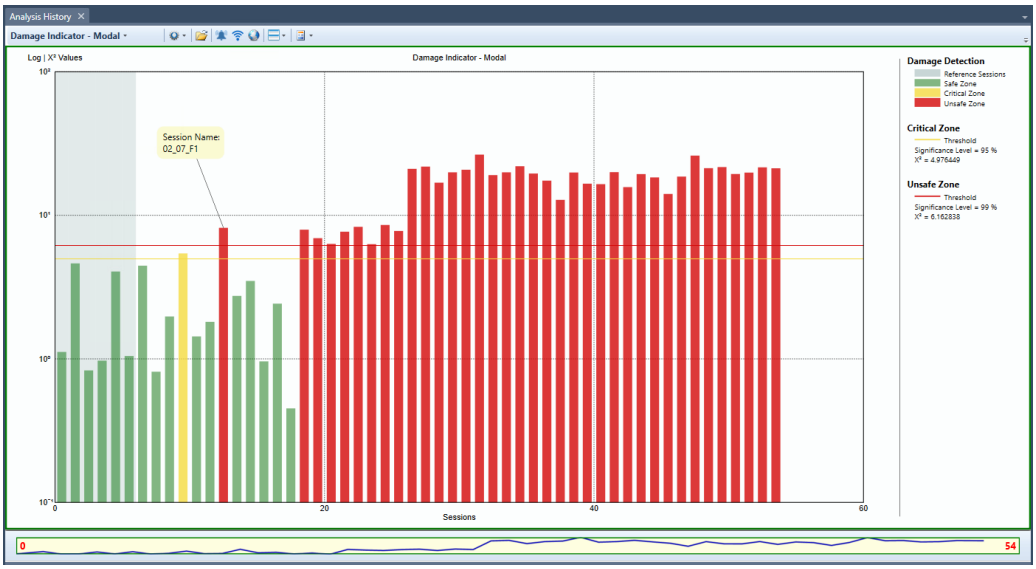

Figure 4. Damage detection with modal parameters (5) using Z24 bridge data

The results of damage diagnosis with the classic subspace residual are studied next. The first 6 data sets are used to obtain the baseline features. The output covariance Hankel matrix of both the reference and the test data set is obtained with $p = 7$ and the reference left nullspace is estimated with $n = 20$. The

covariance of the residual is obtained after the first-order perturbation analysis of the residual, and the sample covariance of the Hankel matrix is computed by splitting data to 200 independent segments. The resultant damage indicators are illustrated in Figure 5. Despite few healthy data sets are classified to critical regions no false alarms occur, and all damage scenarios are detected.

Figure 5. Damage detection with the classic residual (6) using Z24 bridge data

Lastly, the performance of the robust damage detection residual is studied. In this context, the parameters to obtain the baseline and the test features remain the same as in the classic subspace residual. The resultant damage indicators are illustrated in Figure 6. One can observe that while the damage indicators corresponding to the healthy data are classified to the safe region, damage in data sets 21 and 22 is undetected.

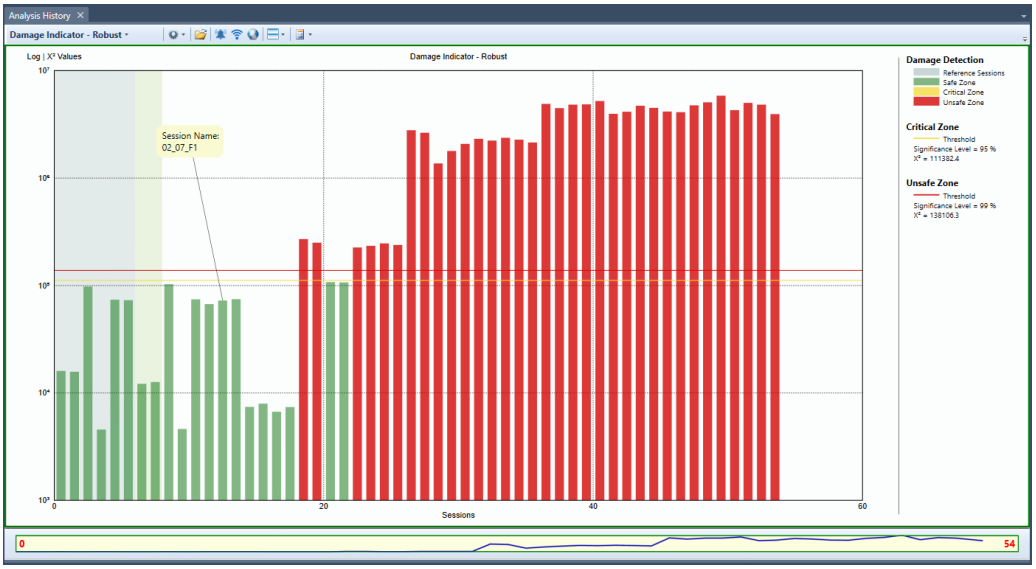

Figure 6. Damage detection with the robust residual (7) using Z24 bridge data

As the studied residuals have different statistical properties, the results also differ. To simplify the decision making about damage and to enhance the performance of the damage detection, the indicators from all the residuals are joined in a Hotelling T2 control chart, which is illustrated in Figure 7. The fusion of the methods in a control chart results in an increased resolution of the damage detection, allowing to distinguish different types of damage, while retaining no false alarms in the healthy state.

Figure 7. Fusion of damage indicators in a Hotelling T2 control chart, Z24 bridge

3.2. S101 bridge

The S101 was a prestressed concrete bridge located in Reibersdorf, Austria. With the main span of 32 m, side spans of 12 m, and a width of 6.6 m, it crossed the national highway A1 Westautobahn. Built in 1960, it had to be demolished due to structural problems and to allow space for additional lanes on the highway underneath. That created an opportunity for conducting progressive structural damage tests. The bridge was artificially damaged and monitored within the Integrated European Industrial Risk Reduction System research project [18].

The measurement campaign was conducted by Vienna Consulting Engineers ZT GmbH (VCE) [19] and the University of Tokyo. The purpose of the campaign was to demonstrate the impact of scientific insight and findings with regards to the rehabilitation measures and cost planning of the transportation infrastructure. Acceleration responses were recorded using 15 triaxial sensors mounted on the bridge deck. The bridge was monitored continuously from the 10th to the 13th of December 2008. A sampling frequency of 500 Hz was used and a total of 714 data sets with 165k samples in each were acquired.

The bridge was closed for any traffic during the progressive damage testing. As a result, the main source of ambient excitation was wind and the vibrations from traffic on the highway beneath the bridge. The structural damages introduced in the bridge were of several types and locations. Two major damage scenarios can be distinguished, as outlined in Table 1.

Table 1. Damage scenarios during the progressive damage test of the S101 bridge

Case 1	Damages	Sets	Case 2	Damages	Sets
A	First cut through the left pier	5	G	Inserting steel plates	45
B	Second cut through the left pier	15	H	2nd tendon cut	178
C	Settlement of the left pier (1st) – 1cm	10	I	2nd tendon cut	178
D	Settlement of the left pier (2nd) – 2cm	21	J	3rd tendon cut	23
E	Settlement of the left pier (3rd) – 3cm	9	K	4th tendon partly intersected	6
F	Lifting the left pier – 6mm	186			

Figure 8. The S101 bridge. Locations of introduced damage are marked in the figure around the north side pier (www.vce.at/iris/)

The first 4 modes obtained with the SSI–UPCX method and tracked across the 681 data sets are shown in Figure 9.

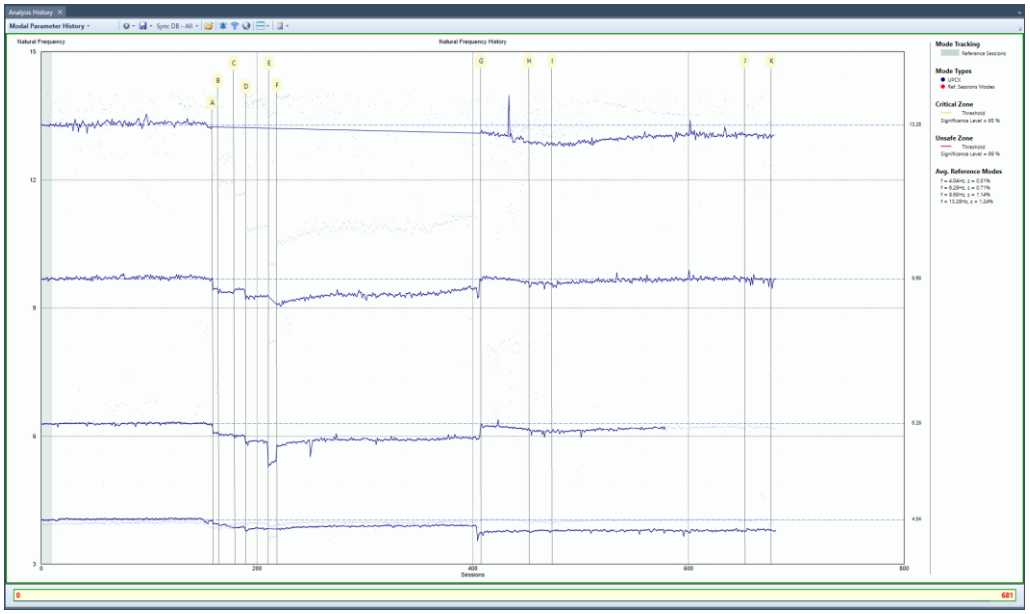

Figure 9. Modal parameters of the S101 bridge tracked across the 681 data sets. Natural frequencies shown

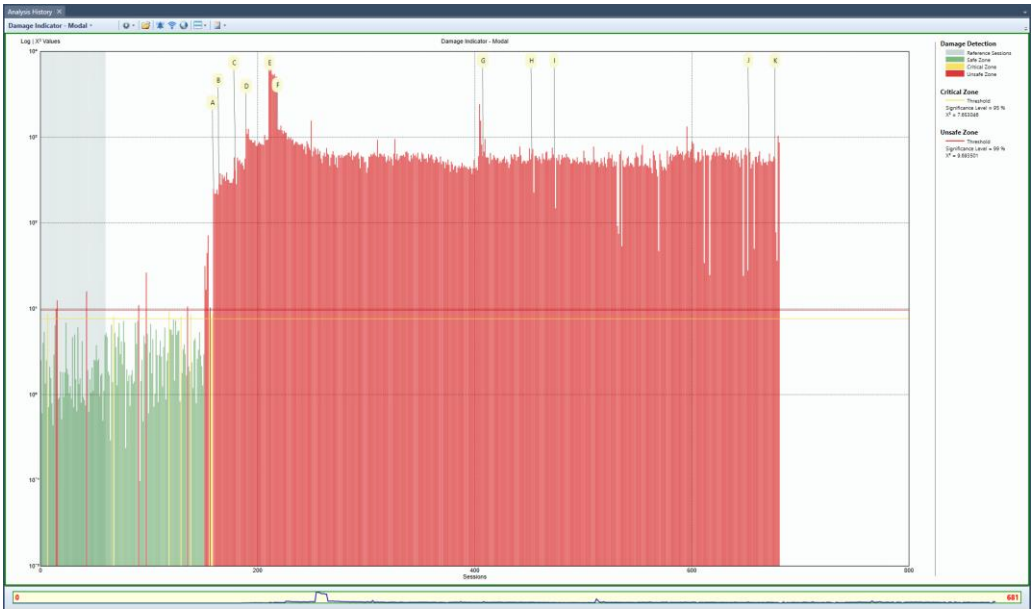

Figure 10. Damage detection with modal parameters (5) using S101 bridge data

The mean values of the corresponding natural frequencies and the mode shape estimates obtained over the first 60 data sets are used to establish a baseline (reference) for the modal parameter-based damage detection (5). The remaining 621 data sets are used for damage testing with the squared Mahalanobis distance (6). The resultant damage indicators are presented in Figure 10. There are a few false alarms in the reference part of the data sets, but there is a significant increase in the damage indicators when damage scenario A is introduced. The damage indicators stay high throughout the remaining data sets.

The results of damage diagnosis with the classic subspace residual are studied next. The first 100 data sets are used to obtain the baseline features. The output covariance Hankel matrix of both the reference and the test data set is obtained with $p = 8$ and the reference left nullspace is estimated with $n = 30$. The covariance of the residual is obtained after the first-order perturbation analysis of the residual, and the sample covariance of the Hankel matrix is computed by splitting data to 200 independent segments.

The resultant damage indicators are illustrated in Figure 11. Despite several false alarms in the reference state, the classic subspace damage indicator reacts heavily when damage is introduced. The results exceed the 99% quantile of the reference distribution for most of the damage cases. However, a small drop between damage cases I and J can be observed. This might be caused by insufficient excitation of the bridge at night.

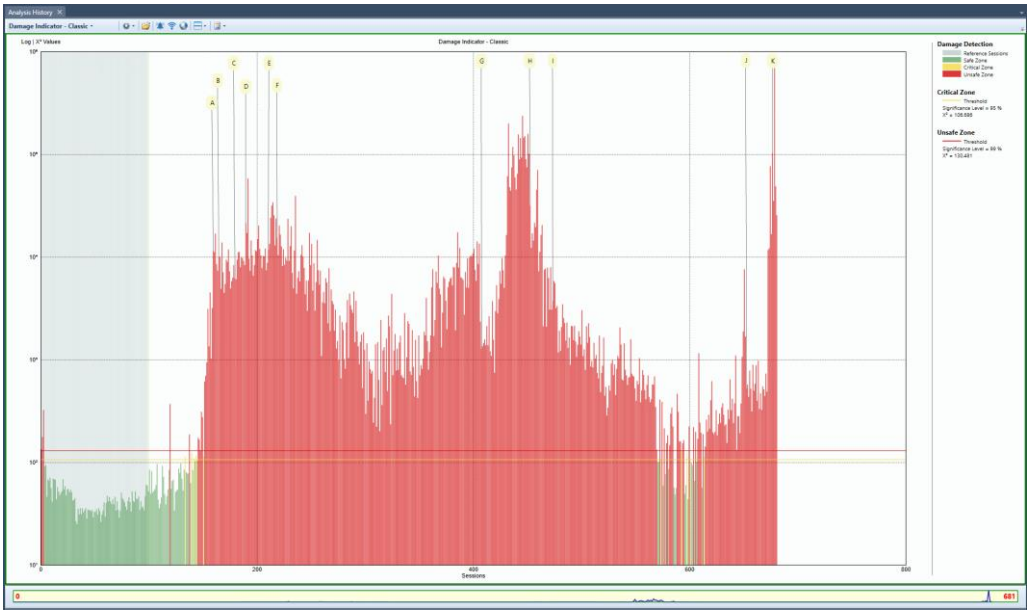

Figure 11. Damage detection with the classic residual (6) using S101 bridge data

The modal parameter-based and classic subspace damage indicators are fused in the control chart shown in Figure 12. The control chart compensates for the drawbacks of each of the two individual damage indicators. There are few false alarms in the reference data sets. However, there is a clear reaction to the damage introduced.

Figure 12. Fusion of damage indicators in a Hotelling T2 control chart, S101 bridge

4. DISCUSSION

The case studies clearly reason for a parallel analysis of multiple damage indicators. Each indicator has its shortcomings, directly related to the statistical properties of the underlying damage diagnosis residual [20]. Consequently, the choice of the method for an SHM system, before the actual analysis is performed, is not trivial. To enhance the reliability of the damage detection and simplify the decision about damage, the fusion of damage indicators in a control chart is beneficial, as demonstrated by the case studies. Additionally, some practical strategies to interpret false alarms can be developed, e.g., by using the fact that false alarms typically do not happen in consecutive data sets. Hence, an alert can be delayed until the next data set is processed, and the alarm occurs again. Furthermore, signal processing techniques exist to remove varying disturbances from the system dynamics by denoising Hankel matrices [21].

5. CONCLUSION

This paper presents a comparative study on three different damage detection residuals, i.e. the classic subspace-based residual, the robust subspace-based residual, and the modal parameter-based residual. To determine the health of structural systems, all three residuals are evaluated in a simple statistical test, which boils down to the squared Mahalanobis distance. The performance of each damage detection residual is compared using data from the Z24 and S101 highway bridges, where the capability of each method to detect the damages and to be ready to deploy in online SHM systems is shown. The fusion of the methods in a Hotelling T2 control chart resulted in the most effective detection of damage. In addition, it was discussed how to interpret and avoid false alarms in SHM systems.

ACKNOWLEDGEMENTS

We thank VCE for providing data from the S101 bridge.

REFERENCES

[1] Ulriksen, M. D., Tcherniak, D., Kirkegaard, P. H., & Damkilde, L. (2016). Operational modal analysis and wavelet transformation for damage identification in wind turbine blades. *Structural Health Monitoring*, *15*(4), 381-388.

[2] Tatsis, K., Ntertimanis, V. K., & Chatzi, E. (2018). On damage localization in wind turbine blades: a critical comparison and assessment of modal-based criteria. In *7th World Conference on Structural Control and Monitoring (7WCSCM)*.

[3] Viefhues, E., Döhler, M., Hille, F., & Mevel, L. (2022). Statistical subspace-based damage detection with estimated reference. *Mechanical Systems and Signal Processing*, *164*, 108241.

[4] Greś, S., Döhler, M., Andersen, P., & Mevel, L. (2021). Subspace-based Mahalanobis damage detection robust to changes in excitation covariance. *Structural Control and Health Monitoring*, *28*(8), e2760.

[5] Teughels, A., & De Roeck, G. (2004). Structural damage identification of the highway bridge Z24 by FE model updating. *Journal of Sound and Vibration*, *278*(3), 589-610.

[6] Kullaa, J. (2003). Damage detection of the Z24 bridge using control charts. *Mechanical Systems and Signal Processing*, *17*(1), 163-170.

[7] ARTeMIS Modal Pro (2022). Structural Vibration Solutions A/S. NOVI Science Park, 9220 Aalborg East, Denmark. www.svibs.com

[8] PULSE Operational Modal Analysis (2022). Hottinger Brüel & Kjær A/S, 2830 Virum, Denmark. www.bksv.com/structuraldynamics

[9] Carden, E. P., & Fanning, P. (2004). Vibration based condition monitoring: a review. *Structural health monitoring*, *3*(4), 355-377.

[10] Döhler, M., & Mevel, L. (2013). Subspace-based fault detection robust to changes in the noise covariances. *Automatica*, *49*(9), 2734-2743.

[11] Basseville, M., Abdelghani, M., & Benveniste, A. (2000). Subspace-based fault detection algorithms for vibration monitoring. *Automatica*, *36*(1), 101-109.

[12] Döhler, M., Mevel, L., & Hille, F. (2014). Subspace-based damage detection under changes in the ambient excitation statistics. *Mechanical Systems and Signal Processing*, *45*(1), 207-224.

[13] Greś, S., Mendler, A., Jacobsen, N. J., Andersen, P., & Döhler, M. (2022, July). Statistical damage detection and localization with Mahalanobis distance applied to modal parameters. In *IOMAC 2022-9th International Operational Modal Analysis Conference*.

[14] Döhler, M., & Mevel, L. (2013). Efficient multi-order uncertainty computation for stochastic subspace identification. *Mechanical Systems and Signal Processing*, *38*(2), 346-366.

[15] Reynders, E., Pintelon, R., & De Roeck, G. (2008). Uncertainty bounds on modal parameters obtained from stochastic subspace identification. *Mechanical systems and signal processing*, *22*(4), 948-969.

[16] Greś, S., Riva, R., Süleyman, C. Y., Andersen, P., & Łuczak, M. (2022). Uncertainty quantification of modal parameter estimates obtained from subspace identification: An experimental validation on a laboratory test of a large-scale wind turbine blade. *Engineering Structures*, *256*, 114001.

[17] Mahalanobis, P. C. (1936). On the generalized distance in statistics. National Institute of Science

[18] Döhler, M., Hille, F., Mevel, L., & Rücker, W. (2014). Structural health monitoring with statistical methods during progressive damage test of S101 Bridge. *Engineering Structures*, *69*, 183-193.

[19] VCE. Progressive Damage Test S101 Flyover Reibersdorf (draft), *Tech. Report 08/2308; 2009*

[20] Mendler, A., Döhler, M. (2022, July). Selection of damage-sensitive features based on probability of detection curves. In *IOMAC 2022-9th International Operational Modal Analysis Conference*.

[21] Greś, S., Tatsis, K., Ntertimanis, V. K., & Chatzi, E. (2022, July). Hankel matrix-based Denoising for Statistical Damage Diagnosis, In *IOMAC 2022-9th International Operational Modal Analysis Conference*.